Impedance Spectroscopy of Nanostructure p-$ZnGa_2Se_4/n$-Si Heterojunction Diode

I.S. Yahia[a,*], M. Fadel[a], G.B. Sakr[a], S.S. Shenouda[a], F. Yakuphanoglu[b,c] and W.A. Farooq[c]

[a]Department of Physics, Faculty of Education, Ain Shams University, Roxy, Cairo, Egypt

[b]Department of Metallurgical and Materials Engineering, Firat University, Elazig, Turkey

[c]Department of Physics and Astronomy, College of Science, King Saud University Riyadh, Kingdom of Saudi Arabia

(Received February 25, 2011; in final form March 24, 2011)

The impedance characteristics of the nanostructure p-$ZnGa_2Se_4/n$-Si heterojunction diode were investigated by impedance spectroscopy method in the temperature range (303–503 K) and the frequency range (42 Hz – 5 MHz). The real and imaginary parts of the complex impedance are changed with the frequency. Both are decreased with increasing temperature at the lower frequencies and are merged at the higher frequencies. The dielectrical relaxation mechanism of the diode was analyzed by the Cole–Cole plots. The Cole–Cole plots under various temperatures exhibit one relaxation mechanism. With increasing temperature, the radius of the Cole–Cole plots decreases, which suggests a mechanism of temperature-dependent on relaxation.

PACS: 84.37.+q, 87.63.Pn

1. Introduction

Defect chalcopyrite compounds with the chemical formula $A^{II}B_2^{III}C_4^{IV}$ contain a crystallographically ordered array of vacancies (stoichiometric voids or vacancies) in the cation sublattice [1, 2]. The low packing efficiency of constituent atoms in lattice facilitates the doping of these compounds by impurities [1, 3]. These ordered vacancy compounds form a bridge between impurity physics and crystal physics [4]. They are a class of materials with high technological interest due to their semiconducting properties, broad band gaps, high optical strength, high photosensitivity and intense luminescence, and potential applications in linear, nonlinear optical and photovoltaic devices [1, 2, 4]. In particular, $HgGa_2S_4$ and $Cd_{1-x}Hg_xGa_2S_4$ are widely used as nonlinear optical materials [5]. Also, tunable filters based on $CdGa_2S_4$ and UV photodetectors based on $CdAl_2S_4$ are already used as devices [4]. $ZnGa_2Se_4$ which is one of these defect chalcopyrite ordered vacancy compounds is a photosensitive material [5]. In addition, it can be used for phase change memories [6]. The electrical properties of $ZnGa_2Se_4$ thin films have been previously studied in our laboratory [7]. Also, we analyzed the current–voltage characteristics of Al/p-$ZnGa_2Se_4$/n-Si/Al nanocrystalline heterojunction diode [8].

Impedance characteristics provide a basic mechanism of electrical properties of the device. While direct current–voltage characteristics of the device give a resistive response, alternating current–voltage characteristics give both a resistive and a capacitive response [9]. The complex impedance spectroscopy is an important tool to analyze the electrical properties and to get more information about the relaxation process of the investigated device [10]. It allows the investigation of intrinsic material parameters such as the frequency dependence of real and imaginary parts of impedance as well as the internal structures of the device [11].

The present paper aims to analyze the complex impedance spectroscopy of Al/p-$ZnGa_2Se_4$/n-Si/Al heterojunction diode. The application of the ac technique of the complex impedance analysis eliminates pseudoeffects, if any, in the material electrical properties by separating out the real and imaginary parts of the material electrical properties. It has unique features to investigate the electrical properties of a material, which are independent of the sample geometrical factors [12]. A Cole–Cole plot, an equivalent electrical circuit, the activation energy ΔE_τ of the relaxation process and the bulk resistance and its activation energy is calculated and interpreted.

* corresponding author; e-mail: `dr_isyahia@yahoo.com`, `dr_isyahia@hotmail.com`, `isyahia@gmail.com`

2. Experimental details

The preparation details of $ZnGa_2Se_4$ film were described elsewhere [8]. The thin film of $ZnGa_2Se_4$ was grown by thermal evaporation technique (Edward's E-306A) onto the n-Si substrate. The silicon substrate was placed on a flat holder rotated horizontally of 3 r/m for the more homogeneity of the film. The distance between source of material and substrate holder was about 20 cm to keep the Si substrates at room temperature to avoid the heating flow to the substrate. The vacuum chamber was pumped up to 2×10^{-5} Torr. The temperature of the compound was then raised, until the whole material is evaporated with a deposition rate of about 2.5 nm/s. Film thickness was controlled by using a thickness monitor (Edward FTM5), and then measured accurately by employing Tolansky's method of multiple--beam Fizeau fringes [13] and it was found to be about 179 nm. The obtained p-$ZnGa_2Se_4$/n-Si was annealed at 700 K for 1 h. Then, Al electrodes were deposited by the thermal evaporation technique using a suitable point contact mask of radius 3 mm. The thickness of Al for the upper and lower electrodes is about 100 nm.

The nanostructure of the $ZnGa_2Se_4$ was confirmed by means of X-ray diffraction (XRD) and atomic force microscope (AFM) in previous work [8]. For XRD analysis of the investigated sample, Philips X-ray diffractometer (model X'-Pert) was used for the measurement by utilizing monochromatic Cu K_α radiation operated at 40 kV and 25 mA. The AFM micrographs were investigated by Park System XE-100E AFM. The analysis of the grain size was done by Park system XEI software. The impedance Z was directly measured by a computer controlled HIOKI 3532-50 LCR meter. The sample temperature was controlled by means of a Lakeshore 331S temperature controller with sensitivity better than ±0.1 K.

3. Results and discussion

The electrical behavior of the diode was studied over a range of frequency and temperature using the complex impedance spectroscopy (CIS). This technique enables us to separate the real and imaginary components of the electrical parameters and hence provides a true picture of the material properties. In order to explain the CIS of the sample, an equivalent circuit for the investigated diode consisting of capacitance C_p and resistance R_p in parallel and both of them are in series with resistance R_s (see Fig. 1).

Figure 2 shows the variation of the real part of impedance Z' as a function of frequency at different temperatures. It is clear that the magnitude of Z' decreases with increasing the applied frequency. The high value at low frequencies is due to the total polarization caused by space charge, dipoles, ions and electrons [14]. At lower frequencies, the Z' value is decreased with increasing temperature, as shown in the inset of Fig. 2 presenting a negative temperature coefficient resistance (NTCR) type behavior. At higher frequencies, the values of Z' merge for all temperatures.

Figure 3 shows the variation of the imaginary part of impedance Z'' with the applied frequency at different temperatures. It is observed that the values of Z'' increase with increasing the applied frequency, until it

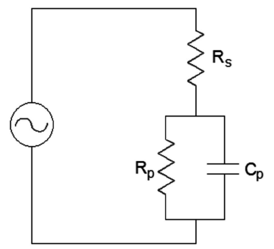

Fig. 1. Equivalent-circuit model for Al/p-$ZnGa_2Se_4$/n-Si/Al HJD.

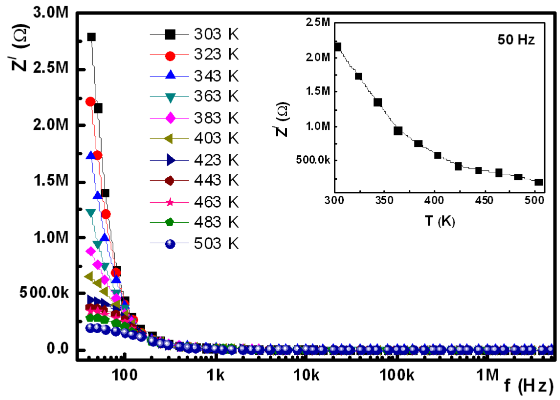

Fig. 2. Frequency dependence of the real part of impedance Z' at different temperatures of Al/p-$ZnGa_2Se_4$/n-Si/Al HJD. Inset: temperature dependence of Z' at 50 Hz.

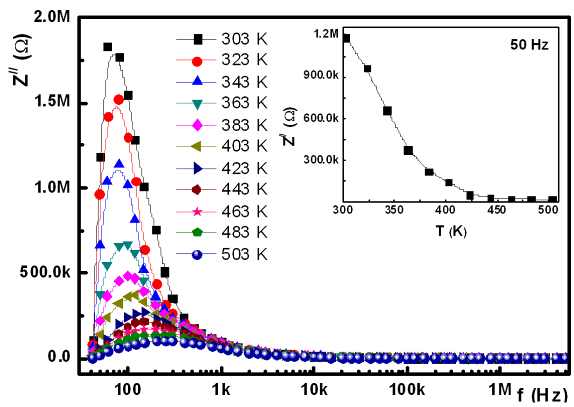

Fig. 3. Frequency dependence of the imaginary part of impedance Z'' at different temperatures of Al/p-$ZnGa_2Se_4$/n-Si/Al HJD. Inset: temperature dependence of Z'' at 50 Hz.

reaches to a maximum peak Z''_{max} and then is decreased with the further increase of frequency. A significant broadening of the peaks with increasing the temperature suggests the existence of a temperature-dependent electrical relaxation phenomenon in the diode. The values of Z'' are decreased with increasing temperature at the lower frequencies, as shown in the inset of Fig. 3. Then, the values of Z'' merge at higher frequencies for all the studied temperatures. The merger of both Z' and Z'' values at higher frequency region may possibly be an indicative of the accumulation of space charge in the device [10, 15]. The peak values of Z''_{max} shifts to the higher frequencies with increasing temperature i.e. the peak frequency f_{max} increases with increasing temperature.

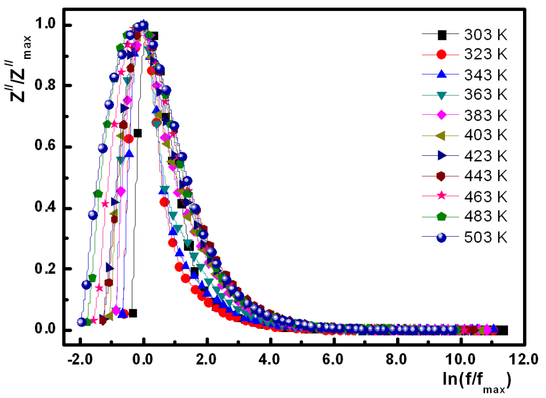

Fig. 4. Scaling behavior of Z'' at various temperatures of Al/p-$ZnGa_2Se_4$/n-Si/Al HJD.

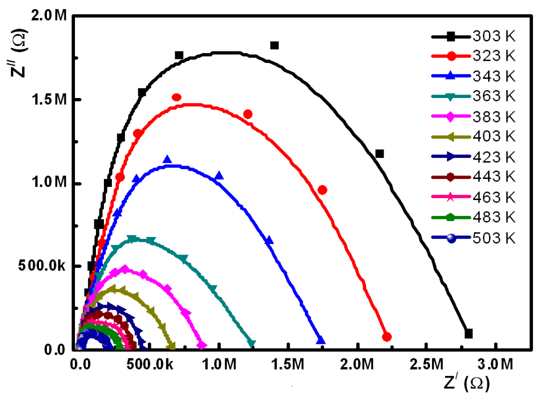

Fig. 5. Cole–Cole plots of Al/p-$ZnGa_2Se_4$/n-Si/Al HJD.

If Z'' is plotted in scaled coordinates, i.e., Z''/Z''_{max} versus $\ln(f/f_{max})$, the entire data of the imaginary part of impedance can collapse into one master curve, as shown in Fig. 4. The scaling behavior of Z'' clearly indicates that the relaxation describes the same mechanism at various temperatures.

For analysis of the relaxation mechanism of the diode, we can use a Cole–Cole plot which explains what kind

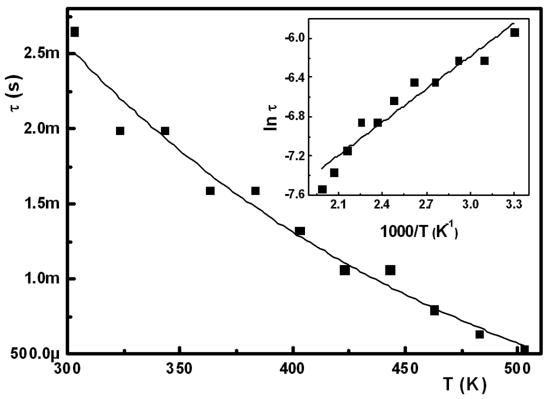

Fig. 6. Temperature dependence of the relaxation time of Al/p-$ZnGa_2Se_4$/n-Si/Al HJD. Inset: $\ln\tau$ versus $1000/T$.

of dielectric relaxation exists in the frequency-dependent response of the device. For this, Cole–Cole plots of the variation of Z'' with Z' over a wide range of frequency at different temperatures were plotted and are shown in Fig. 5. These curves are characterized by the appearance of a single semicircle, which indicates one type of relaxation at all the temperatures. The radius of curvature is decreased with increasing temperature which suggests a mechanism of temperature-dependent on relaxation.

The impedance data is used to evaluate the relaxation time τ of the electrical phenomena in the studied diode. The values of τ were determined from the maximum peak positions of Fig. 3 using the relation, $\omega\tau = 2\pi f_{max}\tau = 1$ [16]. The variation of relaxation time τ with temperature is shown in Fig. 6. As seen in Fig. 6, the value of τ decreases with increasing temperature. At higher temperatures, more electrons are thermally excited, so that the relaxation time of the carrier becomes the shorter [9] and/or the dissipated thermal energy assists formed dipoles to follow the motion of the alternating field [17]. This result confirms the presence of temperature dependent electrical relaxation phenomena in the diode. This variation of τ can be described by the Arrhenius equation as follows [17]:

$$\tau = \tau_0 \exp\left(\frac{\Delta E_\tau}{k_B T}\right), \tag{1}$$

where ΔE_τ is activation energy of the relaxation process and τ_0 is characteristic relaxation time at infinite temperature. The plot of $\ln\tau$ versus $1000/T$ for the studied diode is shown in the inset of Fig. 6. The values of ΔE_τ and τ_0 were calculated from the intercept and slope of the linear fit and found to be 0.098 eV and 6.97×10^{-5} s, respectively.

For a further analysis of the impedance spectroscopy, the bulk resistance R_b and capacitance C_b were determined from the intercept of the semicircle on the Z' axis in Fig. 4. The variation of R_b and C_b with temperature is shown in Fig. 7. It is observed that the R_b value de-

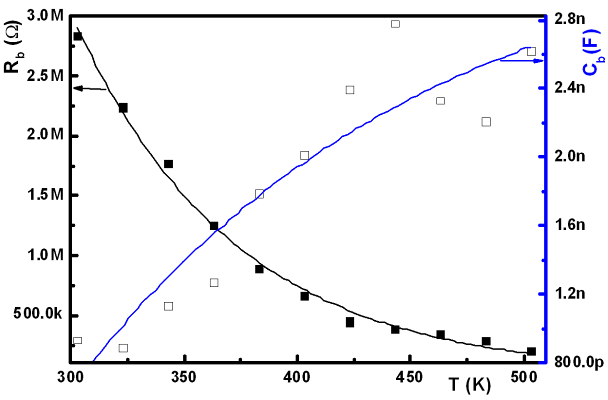

Fig. 7. Temperature dependence of the bulk resistance and capacitance of Al/p-$ZnGa_2Se_4$/n-Si/Al HJD.

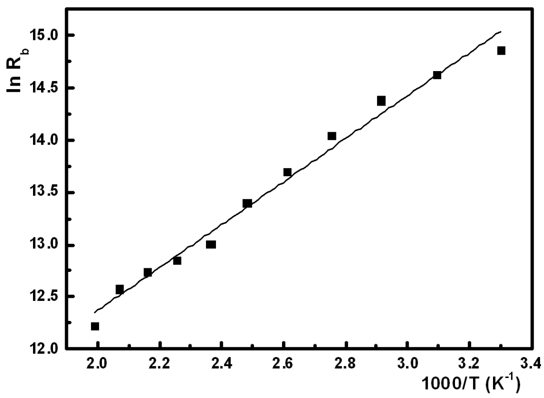

Fig. 8. Plot of $\ln R_b$ versus $1000/T$ of Al/p-$ZnGa_2Se_4$/n-Si/Al HJD.

creases while the C_b value increases with the increase of temperature. The bulk resistance can be described by the following equation:

$$R_b = R_0 \exp\left(\frac{\Delta E_{R_b}}{kT}\right), \quad (2)$$

where ΔE_{R_b} is the conduction activation energy for the relaxation mechanism and R_0 is a constant. Figure 8 shows the plot of $\ln R_b$ versus T. The values of ΔE_{R_b} and R_0 are 0.177 eV and 3.88 kΩ, respectively.

4. Conclusions

Both the real and imaginary parts of impedance are frequency dependent. In addition, they show NTCR type behavior at lower frequencies and merge at higher frequencies. The Cole–Cole plots show the presence of temperature dependent electrical relaxation phenomena in Al/p-$ZnGa_2Se_4$/n-Si/Al heterojunction diode. The appearance of a single semicircle indicates one type of relaxation at all the temperatures. The relaxation time becomes shorter at higher temperatures due to the thermal excitation of more electrons and/or the formed dipoles. The relaxation time and the bulk resistance obey the Arrhenius law with activation energies 0.098 and 0.177 eV, respectively.

Acknowledgments

This work was partially supported by King Saud University under grant: KSU-VPP-102. One of the authors wishes to thank KSU.

References

[1] T. Ouahrani, Ali H. Reshak, R. Khenata, B. Amrani, M. Mebrouki, A. Otero-de-la-Roza, V. Luaña, *J. Solid State Chem.* **183**, 46 (2010).

[2] S. Meenakshi, V. Vijayakumar, A. Eifler, H.D. Hochheimer, *J. Phys. Chem. Solids* **71**, 832 (2010).

[3] Y. Ayeb, T. Ouahrani, R. Khenata, Ali H. Reshak, D. Rached, A. Bouhemadou, R. Arrar, *Comput. Mater. Sci.* **50**, 651 (2010).

[4] J. Xiao-Shu, Y. Ying-Ce, Y. Shi-Min, M. Shu, N. Zhen-Guo, L. Jiu-Qing, *Chin. Phys. B* **19**, 107104 (2010).

[5] A.M. Salem, W.Z. Soliman, Kh.A. Mady, *Physica B* **403**, 145 (2008).

[6] I.S. Yahia, M. Fadel, G.B. Sakr, S.S. Shenouda, *J. Alloys Comp.* **507**, 551 (2010).

[7] M. Fadel, I.S. Yahia, G.B. Sakr, S.S. Shenouda, in: *The 2nd Int. Conf. on Advanced Materials and their Applications and its Workshop on "New Trends on Nanoscience and Laser Physics"*, 2010, NRC, Cairo 2010, p. 107.

[8] I.S. Yahia, M. Fadel, G.B. Sakr, F. Yakuphanoglu, S.S. Shenouda, W.A. Farooq, *J. Alloys Comp.* **509**, 4414 (2011).

[9] J.H. Ahn, J.-U. Lee, T.W. Kim, *Current Appl. Phys.* **7**, 509 (2007).

[10] F. Yakuphanoglu, I.S. Yahia, G. Barim, B. Filiz Senkal, *Synth. Met.* **160**, 1718 (2010).

[11] G.D. Sharma, Dhiraj Saxena, M.S. Roy, *Synth. Met.* **123**, 189 (2001).

[12] Ashok Kumar, B.P. Singh, R.N.P. Choudhary, Awalendra K. Thakur, *J. Alloys Comp.* **394**, 292 (2005).

[13] S. Tolansky, *Introduction to Interferometry*, Longman, London 1955.

[14] S. Kumar Jaiswal, J. Kumar, *J. Alloys Comp.* **509**, 3859 (2011).

[15] K.P. Chandra, K.P. Chandra, K. Prasad, R.N. Gupta, *Physica B* **388**, 118 (2007).

[16] W. Chen, W. Zhu, C. Ke, Z. Yang, L. Wang, X.F. Chen, O.K. Tan, *J. Alloys Comp.* **508**, 141 (2010).

[17] V.S. Reddy, A. Dhar, *Physica B, Condens. Matter* **405**, 1596 (2010).